Ab initio pseudopotential calculation of the equilibrium structure of tin monoxide

Madeleine Meyer,[1] Giovanni Onida,[2] Maurizia Palummo,[2] and Lucia Reining[1]

[1]*Laboratoire des Solides Irradiés, UMR 7642 CNRS/CEA, École Polytechnique, F-91128 Palaiseau, France*
[2]*Istituto Nazionale per la Fisica della Materia, Dipartimento di Fisica dell'Università di Roma ''Tor Vergata,''
Via della Ricerca Scientifica, I–00133 Roma, Italy*

We present an *ab initio* pseudopotential calculation of the structural properties of stannous oxide SnO. We discuss the delicate balance of different contributions to the cohesion of this material, and compare the monoxide to the dioxide SnO_2. We point out how different choices concerning the pseudopotential of tin may dramatically influence the resulting equilibrium structure of SnO, and show that the physically most appropriate choice leads to excellent agreement with experiment.

I. INTRODUCTION

Among the different tin oxides, the most frequently studied one is the stannic oxide SnO_2, due to its technological importance based on possible applications in chemical gas sensors, transparent electrodes, for heat reflection, and catalysis.[1,2] There are different ways of preparing SnO_2, often related to an oxidation of tin passing through the monoxide SnO, which frequently leads to a coexistence of both oxides in the sample. Also an oxygen loss associated with the reduction of SnO_2 may lead to a mixture of SnO and SnO_2, and one extensively studied problem is in fact the distinction between the two oxides by spectroscopic means. The standard technique to obtain information on the oxidation stage would be x-ray photoemission spectroscopy, but it has been shown that this technique is not efficient in the case of the tin oxides, since the change in the free-ion potential between Sn^{2+} and Sn^{4+} is canceled by the change in the Madelung potential at tin sites between the two lattices. Hence, the question is rather approached by detailed studies of the valence band region.[3,4] High-quality experimental results are available, especially for SnO_2, and also theoretical studies have mostly concentrated on SnO_2 (see, for example, Refs. 4–10), whereas only very few works on SnO exist.[11]

SnO, moreover, is an interesting material to study from the theoretical point of view, especially in comparison with SnO_2. Both oxides have a tetragonal structure at room temperature and normal pressure, but whereas SnO_2 exhibits a strong degree of isotropy, with an alternation of tin and oxygen planes, SnO has a layered structure, with two planes of tin atoms facing each other. The cohesion of the SnO_2 crystal is hence easy to understand qualitatively on the basis of electrostatic arguments, whereas this is at first sight not true for SnO.

It is therefore worthwhile to perform a detailed study of the electronic structure, and the resulting crystal structure, of SnO and compare to results obtained on SnO_2.

Recent advances in *ab initio* calculations, mostly density-functional theory local-density approximation (DFT-LDA) applications, allow to determine the ground-state properties and the Kohn-Sham electronic structure[12] for even complicated systems. An efficient scheme has however to be chosen in order to make the calculation of the desired material properties feasible. Since here we concentrate on cohesion and valence band features, it is reasonable to treat the inner shells of the atoms only approximately, and hence to use norm-conserving pseudopotentials and a plane-wave basis set. Tin oxides are *a priori* not the easiest materials to treat in this way. First, it is well known that the *p* component of the oxygen potential is very attractive, due to the lack of a repulsive component in the core. A relatively large basis of plane waves is hence necessary to correctly describe the oxygen. This problem can partially be overcome by the use of soft[13] or ultrasoft[14] pseudopotentials. Second, the tin atom with its 50 electrons is relatively large, which means that (i) relativistic effects have to be taken into account, and (ii) the outer shells of electrons are relatively loosely bound, which implies that the charge density of the atom can be easily distorted by an external perturbation. Moreover (iii), the $4d$ shell has a strong overlap with the $5s$ and $5p$ states, and may be considered as a semicore level. This last kind of difficulty also shows up in more frequently studied, smaller atoms, like gallium, and the exhaustive discussion about how the gallium $3d$ level should be treated in *ab initio* calculation of, e.g., gallium nitride is a good illustration for the complexity of this problem.[15]

The problem (i) is easily solved by including scalar relativistic corrections in the pseudopotentials. In the present work, we will show that the difficulty (iii) can in fact be overcome for the tin oxides, whereas it is extremely important to properly take into account point (ii). We illustrate how drastically the equilibrium geometry can be affected by an improper treatment of this effect, and demonstrate how appropriate choices in the generation and application of the tin pseudopotential lead to excellent agreement with experiment for the ground-state properties of both SnO_2 and SnO.

The paper is organized as follows. In Sec. II we present the structure of SnO and SnO_2, and the computational approach with its technical details used throughout the calculations. In Sec. III we raise the question of the cohesion of SnO, and present a discussion based on the analysis of its charge density, comparing also to SnO_2. This will lead us to consider in Sec. IV some subtleties concerning the choices that have been made for the tin pseudopotential. Finally, Sec. V contains the conclusions that can be drawn from our results.
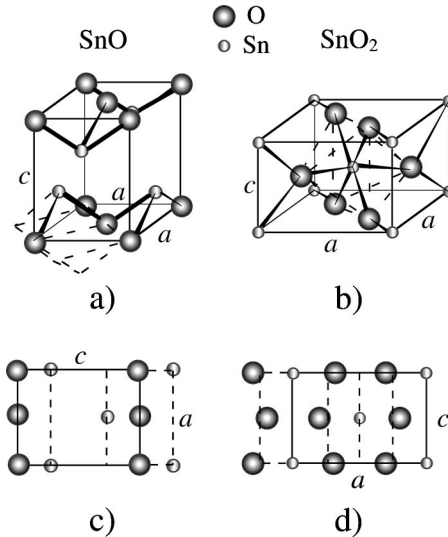
FIG. 1. Crystal structure of SnO (left) and SnO_2 (right). The bottom panels show a projection on the (010) plane. The dashed lines of panels (a) and (b) help to visualize the pyramids [SnO, panel (a)] and oxygen octahedron [SnO_2, panel (b)]. The dashed lines of panels c and d help to visualise the O and Sn planes.

II. METHODOLOGY

The crystalline structures of SnO and SnO_2 are tetragonal at room temperature and normal pressure (Fig. 1) and belong to space groups D_{4h}^7 ($P4/nmm$) and D_{4h}^{14} ($P4_2/mnm$), respectively.[16–18] The difference between SnO and SnO_2 is essentially an additional oxygen plane in SnO_2, which is inserted between two tin planes in the layered SnO crystalline structure [see the projections shown in panels (c) and (d) of Fig. 1]. As a result SnO_2 is a more densely packed crystal where each tin atom is surrounded by a slightly distorted oxygen octahedron [Fig. 1(b)] while in SnO the tin atoms sit on the vertices of pyramids with an oxygen square basis [Fig. 1(a)]. These edge-sharing pyramids form the layers of the SnO structure with tin vertices lying alternatively above and below them. The layers are stacked perpendicularly to the c crystallographic axis with tin atoms facing each other [Fig. 1(c)]. Both crystals are hence described by two parameters a and c for the unit cell (see Fig. 1), and one internal parameter u, the atoms being located at: $O(0,0,0;\frac{1}{2},\frac{1}{2},0)$, $Sn(0,\frac{1}{2},u;\frac{1}{2},0,-u)$ for SnO and $O\pm(u,u,0;u+\frac{1}{2}, \frac{1}{2}-u,\frac{1}{2})$, $Sn(0,0,0;\frac{1}{2},\frac{1}{2},\frac{1}{2})$ for SnO_2, in units (a, a, c).

In order to obtain the theoretical equilibrium geometry, these parameters are determined via total energy minimizations in DFT-LDA. We use norm-conserving,[13,19] fully separable[20] pseudopotentials. For oxygen, they are created according to the scheme proposed by Troullier and Martins,[13] with a core radius of 1.45 bohr for the s and p component, and the atom in its ground state. The p component is used as the local reference component. For tin, we use a potential of the Hamann type[21] (called PP in the following), with the s, p and d component created in an excited state with configuration $[Kr]4d^{10}4f^{0.1}5s^{0.85}5p^{0.85}5d^{0.25}$ (the motivation for this rather complicated choice will be discussed in Sec. IV). The $4d$ electrons are frozen in the core, but nonlinear core corrections are applied.[22] The s component is used as the local reference component. These choices allow us to work at a plane-wave cutoff of 60 Ry. Increasing the cutoff to 80 Ry yields a difference of 100 meV per molecule for the absolute value of the total energy, and leaves the lattice constants virtually unchanged, whereas a further increase to 90 Ry changes the total energy by less than 10 meV. In fact, the final results have been obtained at 80 Ry. We use two special **k** points in the irreducible Brillouin zone (IBZ) for the calculations on SnO_2, and eight special **k** points in the IBZ for SnO. This set of parameters guarantees that the results are not biased by incomplete convergence.

III. COHESION

Using the above parameters, we have minimized the total energy of SnO and SnO_2 with respect to the electronic degrees of freedom, and with respect to the internal lattice parameter u, at fixed a and c. We have performed this calculation for fourteen different configurations ($a,c/a$). We have then fitted the resulting curves with a polynomial of order three, which allowed us to determine the geometrical equilibrium structure. The resulting dependence of the total energy on the crystal volume has then yielded the bulk modulus. The theoretical results are shown in Table. I. For SnO, the comparison of the structural parameters with the experimental data[18] is very good, the largest error being on c/a, which is underestimated by less than 3%. The theoretical cohesive energy turns out to be 9.6 eV/molecule SnO, showing the ususal overestimation of an LDA calculation with respect to the experimental value of 8.6 eV/molecule. The experimental bulk modulus B has been determined from the measured evolution of the lattice parameters a and c under pressure P given in Ref. 18 according to $B=-V_0 dP/dV$, where V_0 is the equilibrium volume. One finds $B_{exp}=48\pm5$ GPa. The theoretical value (45 GPa) is obtained directly from the relation $B=V_0 d^2E/dV^2$. For SnO_2, the agreement of the calculated structural parameters is even better, the largest error being less than 2% (still on c/a). As for the

TABLE I. Ground-state properties of SnO and SnO_2. In parenthesis, the experimental values from Refs. 18 (SnO, structural properties), 23 (SnO_2, structural properties), 27 (SnO and SnO_2, cohesive energy), and 28 (SnO_2, B). For the experimental value of B of SnO, see text.

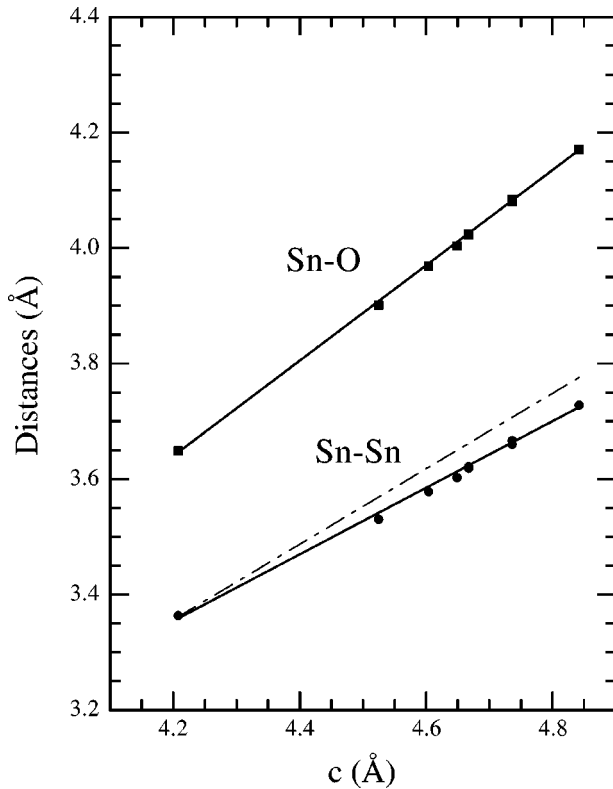|	a (Å)	c/a	u	E_c (eV)	B (GPa)
SnO	3.76 (3.799)	1.238 (1.2706)	0.244	9.6 (8.6)	45 (48±5)
SnO_2	4.74 (4.737)	0.66 (0.673)	0.307 (0.307)	15.5 (14.4)	218 (208)

FIG. 2. Second-neighbor interatomic distances in SnO as a function of c, the lattice parameter controlling the interlayer distance. The dot-dashed line represents the purely geometrical curve obtained if the internal atomic position of Sn is not allowed to change.

cohesive energy, we obtain a value of 15.5 eV/molecule SnO_2, to be compared with the experimental value of 14.4 eV/molecule. Also the calculated bulk modulus $B_{theo} = 218$ GPa is in good agreement with the value of $B_{exp} = 208$ GPa, which can be extracted from the measured elastic constants C_{ij} via the relation $B = (C_{11}C_{33} + C_{12}C_{33} - 2C_{13}^2)/(2C_{33} + C_{11} + C_{12} - 4C_{13})$. This relation, appropriate for our case of D_{4h} symmetry, results from the compressibility $\kappa = 1/B$.[24] This agreement is also consistent with other findings in the literature.[8,9]

We can now look in detail at the cohesion of SnO. This oxide has a markedly layered structure, and it is worthwhile to study the nature of the binding between the layers. It cannot be understood by simple electrostatic arguments, since two layers of positively charged tin atoms are facing each other. Figure 2 shows the evolution of the second-neighbor distances in SnO, as a function of the lattice parameter perpendicular to the layers, c. Sn and O atoms are next neighbors in the *same* plane, but regarding the interlayer cohesion we are rather interested in distances between atoms on neighboring planes. In fact, in this case the shortest distance is always between two tin atoms, for all values of c. The dot-dashed line in Fig. 2 gives the evolution of these Sn-Sn distances d_{Sn-Sn} in function of c, which one would obtain by freezing the atomic positions of the atoms in each layer and by simulating the compression only through a variation of the distance between the two layers. The starting configuration chosen is the one that minimizes the total energy for a

$= 3.799$ Å and $c/a = 1.1074$, which leads to a distance of the Sn atom with respect to the next oxygen plane of $z(Sn) = 1.0912$ Å. This purely geometric curve is then given by $d_{Sn-Sn} = \sqrt{2(a/2)^2 + (c - 2z(Sn))^2}$. It deviates from the curve that one actually observes when the position of the tin atom $z(Sn)$ is allowed to vary during the minimization (full circles). In fact, since the tin atoms repel each other this latter curve shows a smaller slope than the purely geometric one: this attempt to maximize the distance between tin atoms is obviously favorable for electrostatic reasons. Still, d_{Sn-Sn} is at all distances considerably smaller than the distance between the second-neighbor tin and oxygen atoms, i.e., between a tin atom and the next oxygen atom in the plane facing the tin atom. This distance d_{Sn-O}, which includes a minimization with respect to the internal parameters (hence the equivalent to the full circles in the case of d_{Sn-Sn}), is given by the filled squares. For decreasing values of c, d_{Sn-Sn} and d_{Sn-O} get closer, but for the interplane distances in the range of interest d_{Sn-Sn} is always smaller than d_{Sn-O}. In a naive approach, neighboring layers should hence repel each other. This is of course not the case, but it is clear that the interlayer binding must be a delicate balance with a resulting relatively weak force. Indeed we find that the compressibility perpendicular to the planes is almost one order of magnitude smaller than the one we obtain in the in-plane direction.

In order to examine this situation, it is worthwhile to study the charge distribution in SnO, and to compare it to the charge distribution of SnO_2. The three-dimensional (3D) densities of charge, calculated at the experimental atomic configuration, are plotted in Fig. 3. One level is used in each figure, and its intensity for SnO and SnO_2 is chosen such that the ratio between the two intensities is the same as the ratio between the average densities of SnO and SnO_2.

A simple look at the charge-density distribution of SnO_2 in the [010] direction [Fig. 3(a)] shows that its cohesion is easy to understand in terms of electrostatics. For SnO, a closer look at the graphs is necessary. The left panel in Fig. 3(b) shows in fact an isotropic distribution, because we are looking at a projection on a (001) plane, i.e., on top of a layer. In the right panel in Fig. 3(b) we are looking perpendicularly to the layers, and this projection on a (010) plane shows clearly the difference with SnO_2 in Fig. 3(a). In fact, we can see the tin atoms facing each other on a diagonal. The interesting fact is that ''hats'' of charge covering the Sn atoms appear, which screen the Sn ions and decrease the repulsive forces. This effect can be better illustrated when looking at a projection on a ($\bar{1}10$) plane, and compressing the material perpendicular to the planes, at a fixed value of a. This is done in Fig. 3(c): the right panel has been calculated at the experimental atomic configuration, whereas the left panel has been obtained by decreasing c by about 13%. The ''hats'' show a tendency to be more intense for the smaller interplane distance, in order to increase the screening effect, which allows for interlayer cohesion.

IV. DETAILS OF THE PSEUDOPOTENTIAL APPROACH

One might wonder whether the visibly very strong distortion of the charge density close to the tin ions has any con-
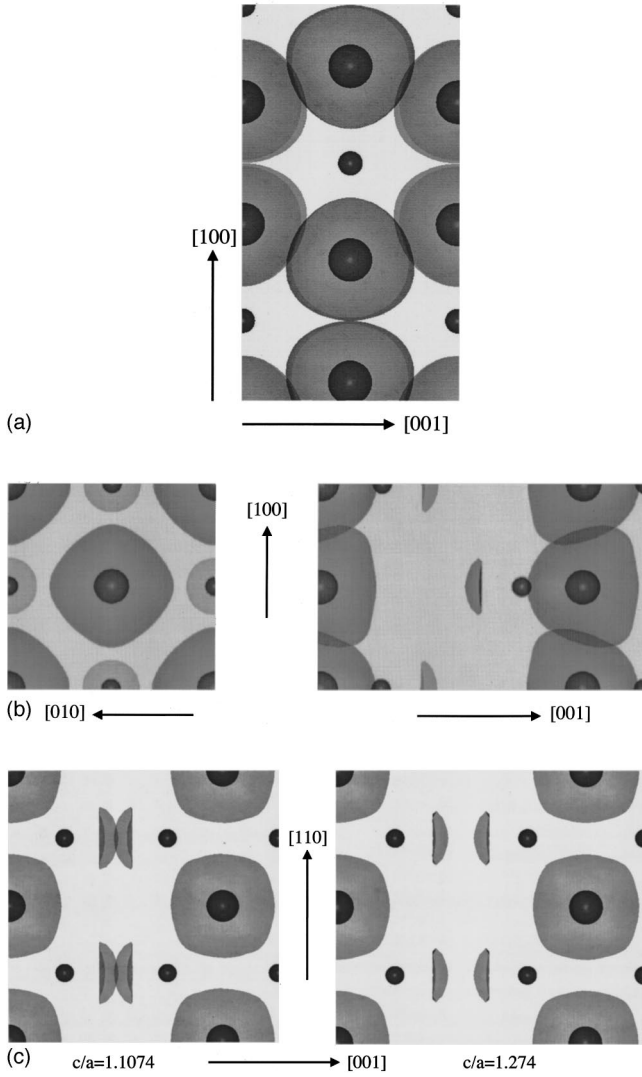
(a)

[100]

[001]

(b) [010]

[100]

[001]

(c)   c/a=1.1074

[110]

[001]   c/a=1.274

FIG. 3. Charge-density isosurfaces for SnO_2 (0.069 electrons/bohr^3) (a) and SnO (0.044 electrons/bohr^3) [(b) and (c)]. 3D surfaces are projected along the indicated crystallographic directions. In part c, the left panel corresponds to a c/a ratio reduced by about 13% (see text). The dark grey spheres correspond to oxygen (larger ones) and tin (smaller ones).

sequences for the calculations. In order to quantify this distortion, we have projected the wave functions of the crystal onto contributions of given angular momentum contained in spheres centered on the tin atoms. The results can then be compared to those of a free tin atom where, for our choice of the core-valence separation, angular momenta higher than p do not contribute at all.

The results are shown in Fig. 4, where the contributions to the valence charge density coming from the projections of the crystal wave functions with s, p, d, and f symmetry are shown on the right part of the graphs. They are represented as a function of the radius of the integration sphere. For comparison, on the left vertical axis the s-, p-, and d-radial components of the tin pseudopotential are also shown. Figure 4(a) refers to SnO, and Fig. 4(b) to SnO_2.
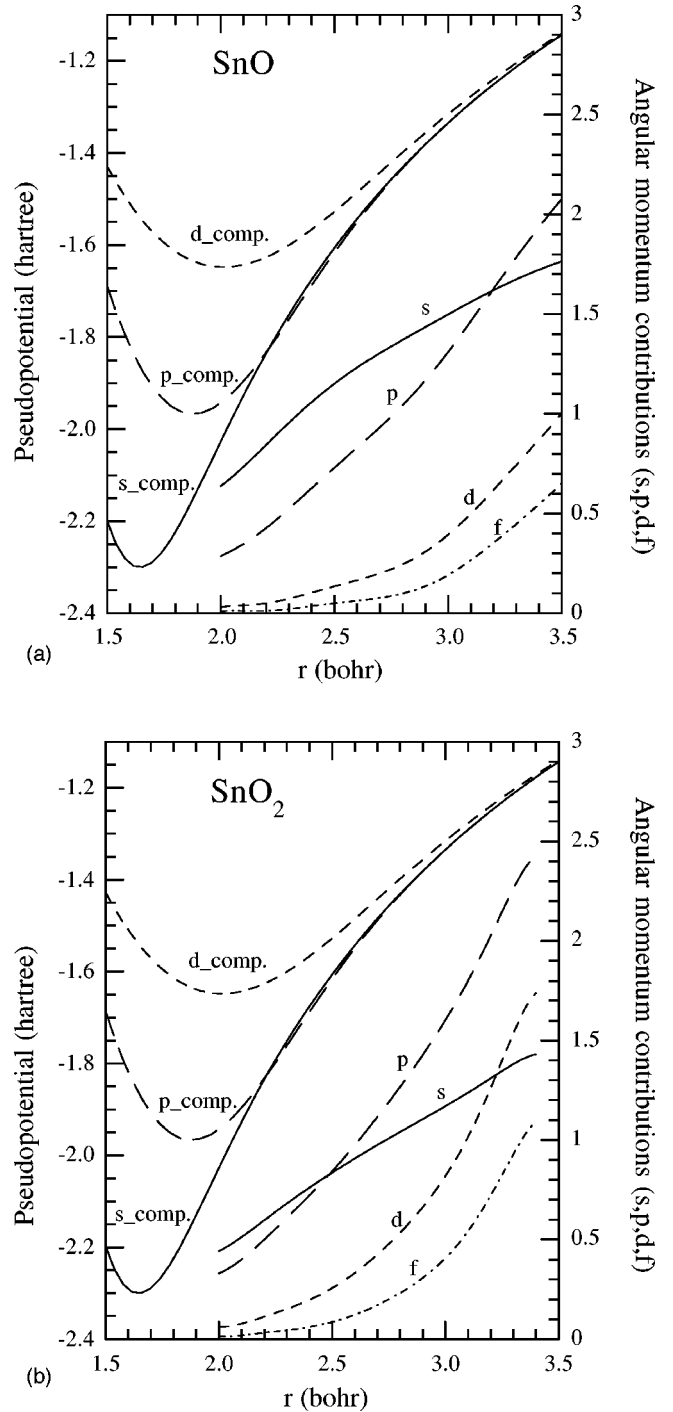
When observing the projections it turns out that obviously

(a)

(b)

FIG. 4. Panels (a) and (b) refer to SnO and SnO_2, respectively. In each panel, right part: contributions to the valence charge density coming from angular momentum (s,p,d,f) decomposed wave functions of the crystal, plotted versus the radius of a sphere centered on the tin atom. On the left part, the different l components of the pseudopotential are shown.

higher angular momenta gain in importance with increasing sphere size. The important point is, however, that at a radius, which is physically meaningful, like $r = 3$ bohr, the contribution of the f component is already significant. This might have consequences for the pseudopotential calculation. In fact, if the f component is important, the potential acting on

that component becomes important, too. A look at the pseudopotential components drawn in the same figure shows that indeed at distances around $r=3$ bohr the s, p, and d components are still different, which means that they may give different contributions to the total energy when they are chosen as the local reference component (see below), and hence implicitly applied to a state of f symmetry.

We shall therefore have a closer look at the importance of the local reference component used for the pseudopotential of the tin atom.

Very often, one starts with a calculation that can be called ''standard'': one creates the pseudopotential freezing the core in its ground state for all components (even those created in an excited state), and uses the component with the largest l to be the local reference component, i.e., the d channel for the case of tin. Taking the ''largest l'' component as local reference component has the obvious advantage that it simplifies the calculations. It has however to be justified. Let us therefore recall the basic ideas involved in the choice of a local reference component.

The pseudopotential as obtained from the atomic calculation is in principle built up by an infinite sum of projections onto angular momenta:

$$V^{ps} = \sum_l V_l^{ps}(r)|l\rangle\langle l| \tag{1}$$

Making use of the facts that the radial components $V_l^{ps}(r)$ become equal to each other starting from some distance r, that atomic wave functions of increasing angular momentum are centered increasingly far from the atom, and that moreover even in the solid close to the atoms higher angular momenta are less important than the ones that are present in the atomic ground state, one can choose an angular momentum l_{max} such that $V_l^{ps}(r) \simeq V^{loc}$ for every $l > l_{max}$. The sum over Eq. (1) can hence be rewritten as

$$V^{ps} = \sum_{l=0}^{l_{max}} V_l^{ps}(r)|l\rangle\langle l| + V^{loc}\sum_{l=l_{max}+1}^{\infty}|l\rangle\langle l| \tag{2}$$

and using the completeness relation $\Sigma_{l=0}^{\infty}|l\rangle\langle l|=1$, one has

$$V^{ps} = V^{loc}(r) + \sum_{l=0}^{l_{max}} \Delta V_l^{ps}(r)|l\rangle\langle l| \tag{3}$$

with $\Delta V_l^{ps}(r) = V_l^{ps}(r) - V^{loc}(r)$. Of course, the local reference component $V^{loc}(r)$ must be chosen such that it reproduces the scattering properties of the potential for $l > l_{max}$ in an optimum way.

Very often, and also in our case, the nonlocal part of the pseudopotential $\Sigma_{l=0}^{l_{max}}\Delta V_l^{ps}(r)|l\rangle\langle l|$ is further modified by transforming it into the fully separable form proposed by Kleinman and Bylander (KB).[20] This requires additional care in the choice of the reference component, since the latter determines the nonlocal part of the potential that is to be transformed. A bad choice may strongly degrade the results, and even lead to the appearance of unphysical ghost states.[25] Since this problem is well known, generally the choice of the reference component is made on the basis of the quality of

the KB transformation, and much less attention is paid to the problem of how well this component reproduces the higher angular momenta.

In the case of the tin atom, and with the creation scheme described in Sec. II, the choice of the reference component is also suggested by KB problems, since a local d component yields logarithmic derivatives that are of bad quality in the range of the empty states not too far from the Fermi level. However, this is not the only problem linked to the reference component, as we will show in the following.

We have in fact also carried out calculations using another pseudopotential (called HB in the following), created using the Hamann scheme and according to the following prescription: the s and p components are created in the ground state, and the d component is created in the excited configuration proposed in Ref. 19, namely $[Kr]4d^{10}5s^{1.0}5p^{0.75}5d^{0.25}$. The default core radii of 1.1, 1.3, and 2.0 bohr for the s, p, and d component, respectively, are used. The core charge, with a model core radius of 0.75 bohr, is frozen in the ground-state configuration. Figure 5(a) shows the logarithmic derivatives for that pseudopotential, using the d component as the local reference component. The agreement between the all-electron result, the semilocal pseudopotential result and the separable KB one in the energy range of interest around the Fermi level is very good concerning the semilocal form, and also acceptable concerning the separable one. In order to complete the illustration of the quality of this pseudopotential, we have performed calculations of the eigenvalues of an isolated tin atom in different strongly excited configurations, which are described by the quantum numbers and occupations listed in the first three columns of Table II. The fourth column shows the results of all-electron calculations, performed with a frozen core that is obtained from a ground-state calculation. These are the results that should be directly compared to the results of the HB pseudopotential, shown in column 5, which has been created with the same core. (For the sake of completeness, we show the same comparison also for the PP pseudopotential used throughout the calculations, in Table III. In that case, in the all-electron calculations the core is frozen in the excited state used to create the pseudopotential.) The agreement between the all-electron frozen core and both pseudopotential results is good. We have also explicitly checked that the atomic eigenvalues calculated using the KB form are close (within less than 10 meV) to the ones using the semilocal pseudopotential. Moreover, for the HB and similar pseudopotentials, we have performed calculations on the solids with and without using the separable form proposed by Kleinman and Bylander,[20] and did not find significant differences concerning total energies. Absolute values of the total energies have in fact changed by less than 100 meV.

We should hence expect that using the HB potential the separable form of the pseudopotential should not introduce a relevant dependence of the results on the choice of the reference component. However, there *is* indeed a significant influence of the reference component on the results: using the HB pseudopotential, we obtain (at various fixed geometries) a difference in total energy of the order of 3 eV, between the results obtained with a local s, or with a local d component. This is of course unacceptable, since changes in
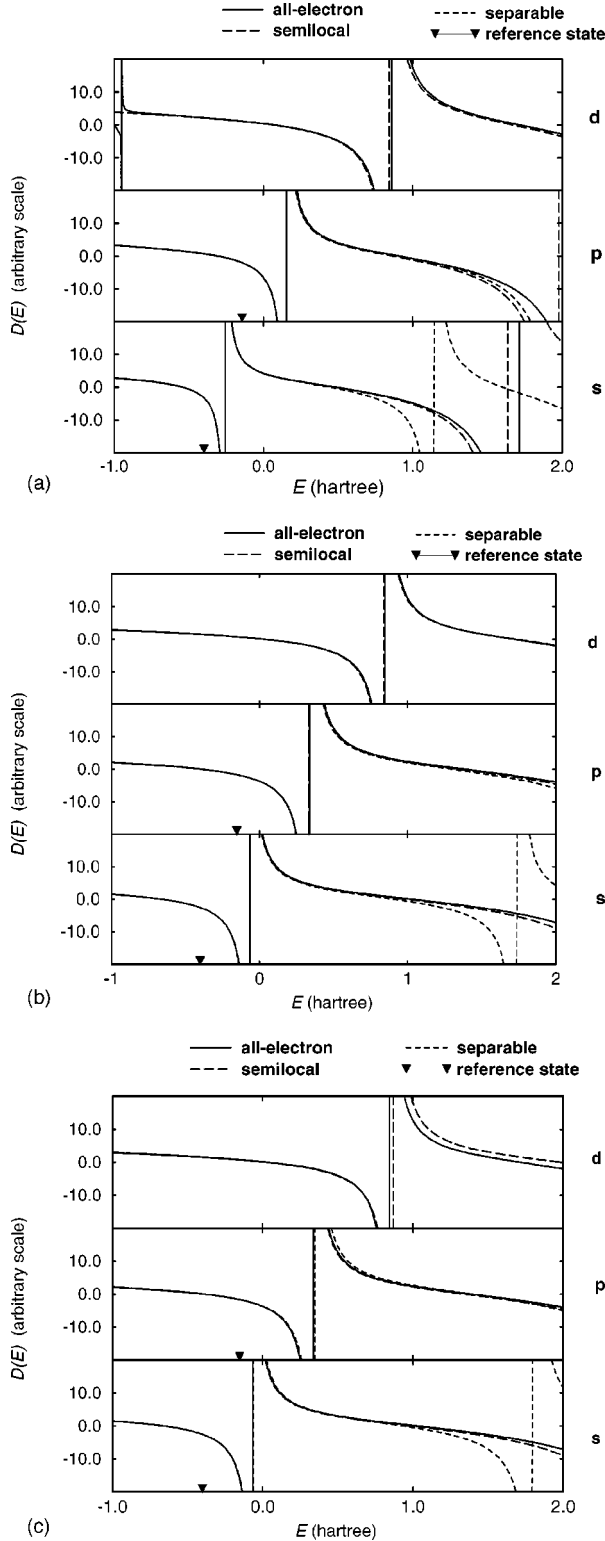
(a)

(b)

(c)

FIG. 5. (a) Logarithmic derivatives of the tin HB pseudopotential (see text) using the d component as local reference potential. Full line: all-electron; long-dashed line: semilocal pseudopotential; dashed: separable KB pseudopotential. The black arrows indicate the energy of the reference state used in the Hamann scheme.[21] (b): Same, for the ''hard'' pseudopotential of Silicon; (c): same, for the ''soft'' pseudopotential of silicon (see text and caption of Fig. 6).

TABLE II. Tin atom eigenvalues in different excited configurations: comparison between all electron calculations, with the core frozen (AE-CF) in the ground state, and the HB pseudopotential.

	n	l	Occupation	AE-FC (eV)	HB(eV)
Conf1	5	0	2	−10.8150	−10.8150
	5	1	2	−3.8737	−3.8737
	5	0	1.00	−28.2263	−28.1730
Conf2	5	1	0.75	−19.5376	−19.5091
	5	2	0.25	−9.5960	−9.5953
	5	0	1.00	−28.6702	−28.6050
	5	1	0.75	−19.9457	−19.9095
Conf3	5	2	0.10	−9.9278	−9.9240
	6	0	0.10	−10.2050	−10.2260
	4	3	0.10	−5.0792	−4.8085
	5	0	0.85	−28.3047	−28.3151
Conf4	5	1	0.85	−19.5722	−19.6009
	5	2	0.25	−9.5952	−9.6297

the total energy due to a different reference component are not canceled by a change in the total energy of the pseudoatom, and remain hence as errors on physical quantities like the cohesive energy. This fact confirms a finding of a previous preliminary study of tin oxides, where we had been using a similar pseudopotential and a local d component, and obtained large errors on the equilibrium geometry, in particular an underestimation of c by as much as 11%.[11] That pseudopotential (called BHS in the following) was the one proposed in the original paper of Bachelet, Hamann, and Schlüter.[19] It is very similar to the HB one, and we have in fact checked that it yields total energy differences, which are very close to those obtained with the latter. ''Very close'' means here that when we calculate total energy differences ΔE_{tot}, either between two different geometries or between two different reference components, the BHS and HB pseudopotentials yield

TABLE III. Tin atom eigenvalues in different excited configurations: comparison between the PP pseudopotential and all-electron calculations, with the core frozen in the configuration used to create PP.

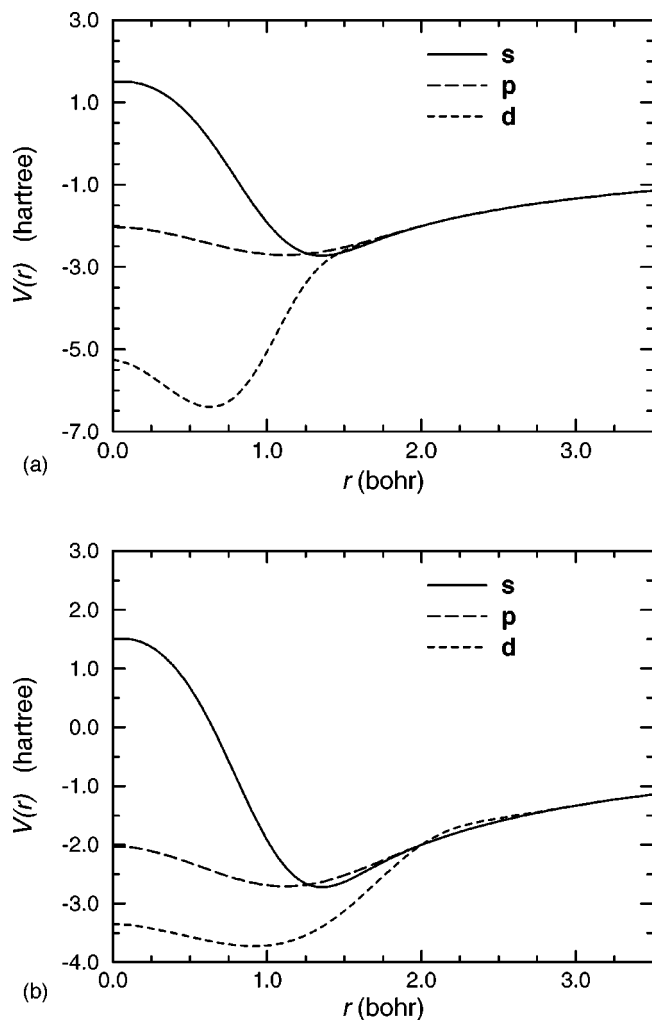|	n	l	Occupation	AE-FC (eV)	PP(eV)
Conf1	5	0	2	−10.6786	−10.6999
	5	1	2	−3.8316	−3.8454
	5	0	1.00	−27.9361	−27.9363
Conf2	5	1	0.75	−19.3462	−19.3474
	5	2	0.25	−9.5354	−9.5399
	5	0	1.00	−28.3731	−28.3627
	5	1	0.75	−19.7473	−19.7419
Conf3	5	2	0.10	−9.8613	−9.8636
	6	0	0.10	−10.1632	−10.1839
	4	3	0.10	−5.0731	−5.0731
	5	0	0.85	−28.0156	−28.0156
Conf4	5	1	0.85	−19.3818	−19.3818
	5	2	0.25	−9.5360	−9.5360

FIG. 6. Silicon pseudopotential created with the Hamann scheme[21] and using the standard configuration proposed in Ref. 19. The core radii for the s, p, and d components are 1.0, 1.3, and 0.96 bohr in panel (a) ''hard,'' while in panel (b) r_d has been increased to 1.5 bohr ''soft.''

results ΔE_{tot}^{BHS} and ΔE_{tot}^{HB}, where $|\Delta E_{tot}^{BHS} - \Delta E_{tot}^{HB}|$ is at least one order of magnitude smaller than ΔE_{tot} itself. Our detailed analysis for the HB pseudopotential should hence also apply to the BHS one, which confirms again that indeed the choice of the reference component is critical and can lead to very bad results as those of Ref. 11, even when there is no problem with the KB separation.

These findings are not in contradiction with the generally good results that are obtained on other materials using any ''good'' (i.e., without problems due to the KB scheme) reference component. In order to illustrate this point, we have created two pseudopotentials for silicon. They are created in the Hamann scheme, and using the configuration proposed in Ref. 19 for the various components. The first ''hard'' one has core radii $r_s = 1.0$, $r_p = 1.3$, and $r_d = 0.96$ bohr, and the second ''soft'' one has $r_s = 1.0$, $r_p = 1.3$, and $r_d = 1.5$ bohr. The two pseudopotentials are shown in Fig. 6(a) and 6(b), respectively, and their logarithmic derivatives are shown in Fig. 5(b) and 5(c).

The difference of the logarithmic derivatives is such that it would be very hard to deduce any significant influence on the transferability of the pseudopotential, in particular for ground-state calculations, with a slight preference for the option ''soft.'' The overall results are qualitatively very similar to those of the tin atom. However, performing total energy calculations for bulk silicon with the hard pseudopotential we have found that changing the reference component from d to s leaves the lattice constant unchanged, and increases the absolute value of the total energy by only 50 meV. In fact, there is a major difference with tin oxide: a look at the hard pseudopotential in Fig. 6(a) shows that already at $r = 2$ bohr the different components are indistinguishable; second, at this distance the analysis of angular momentum contributions in bulk silicon reveals no significant presence of the f channel yet. This explains why bulk silicon with this pseudopotential is not sensitive to a change in the reference component, but SnO is indeed. Instead, a situation similar to the one of SnO is reproduced when we use the soft pseudopotential. Figure 6(b) shows that the components are now different up to $r = 2.8$ bohr. In fact, the total energy calculations on the solid yield results, which differ by as much as 0.5 eV when changing the reference component from s to d, and which also show a change in the lattice constant of 1.3% due to the change of the reference component. The problem does hence also exist in silicon when a soft (i.e. rather standard) pseudopotential is used, although to a much lesser extent than in SnO.

One could be tempted to explain the strong f contribution around the tin atom in SnO with the particularly nonisotropic structure of this material. However, this hypothesis is easily eliminated by an analysis of the charge density of SnO_2, which is a very isotropic material. The result is shown in Fig. 4(b). It turns out that the behavior is very similar to that of SnO. In particular, also in SnO_2 at distances around $r = 3$ bohr the f component starts to be visible. Hence, for both oxides the choice of the reference component should be important.

This is in fact the case: performing a ground-state calculation for SnO_2 with the d component as the local reference, the results are still reasonable when compared to the experimental values, but significantly different from the results listed in Table I: in particular, the theoretical equilibrium parameter a turns out to change from $a = 4.74$ Å to $a = 5.05$ Å, whereas the ratio c/a is stable.

It would of course not be very satisfactory to conclude that the ''best'' reference component is simply the one yielding the best agreement between theoretical and experimental results. However, more evidence is given by performing calculations on the isolated tin atom. Using the code of Ref. 26, we have studied total energies, eigenvalues and pseudo-wave functions of the tin atom in different excited states including bound f states, using a pseudopotential with four components (s to f). The last component was either a true f component created according to the scheme of Hamann,[21] with the atom in its ground state and a core radius of 1.8 bohr, or one of the other three lower components. In that way, we can simulate the role of the reference component in the solid. We have verified that, whereas using the true f component as the ''ref-

erence'' component yields generally very good eigenvalues for the f level (which simply means that the pseudopotential is transferable), this is not always true for the other choices for the forth component. In particular, the d component yields the worst results, whereas the choice of s as the ''reference'' component yields results that are the closest to the ones obtained with the f component. Of course, these tests on the isolated atom will have a tendency to overestimate the effects, and cannot give any quantitative insight concerning the solid, but we believe that they well illustrate the tendencies, and that we can in fact conclude that the s component is the best substitute for the true f component. We have verified this fact further by performing calculations on SnO_2 at various geometries, using the s, p, d, or f component as local reference component. We find that for all examined geometries a local s component gives the results which are the closest to the ones obtained with a local f component (a typical error on the absolute total energy is of the order of 0.3 eV, and energy differences are well reproduced), whereas the performance of the p component as the local reference one is slightly worse, and a local d-component yields results that are different by up to 5 eV.

These numerical results add to the fact that (i) it is reasonable to assume that, when the potential adapted to the f orbitals is not available, the s component best simulates a sort of spherical average, right as in tight binding calculations an s^* orbital can replace the set of d orbitals and that (ii) as pointed out already in Ref. 19, since the d component refers to a state that is not bound in the ground state of the atom, it bears the biggest arbitrariness. In the case of silicon, it turns out that this arbitrariness induces changes in a region close to the core, that is not relevant for cohesion, whereas this is not true for the tin oxides.

The above discussion and comparison with experiments draw validity from the assumption that the $4d$ electrons can in fact be treated as core electrons. This choice is of course strongly suggested by practical reasons, especially in view of the fact that treating the d electrons of a given shell n as valence electrons may impose to treat also the ns and np electrons as valence electrons, which is generally not feasible in a plane-wave calculation without making compromises on the numerical quality of the results. On the other hand, several studies on tin oxides[6,7] have shown that there is only very few hybridization of the Sn $4d$ states with other states. Nevertheless, the question whether the only loosely bound Sn $4d$ electrons can really be frozen in the core should be treated with care. Tests on the isolated Sn atom suggest in fact that the $4d$ electrons *do* relax when the valence shell is perturbed, as it will be the case in the solid. This becomes clear from a comparison of the all-electron results of Table II and Table III, respectively. The only difference between these results is the excitation of the core. The differences are significant. Again, it would be an exaggeration to extrapolate results from the tests on the isolated atom to quantitative results for the solid, but these findings suggest that the relaxation of the Sn $4d$ states may have *some* influence on the results. In order to include this fact as much as possible in our calculations, we have tried to simulate the perturbation of the Sn 4d states in the solid via the pseudopotential: we

have in fact performed a first set of calculations on the solid by using a pseudopotential created with the core frozen in its ground state. We have then analyzed the charge distribution in the solid, by projecting the states on the components of the different angular momenta within spheres around each atom. We have chosen the spheres such that the radius of the sphere around an oxygen atom is roughly half of the distance between neighboring oxygen atoms, and that the total charge contained in the spheres around the tin and oxygen atoms equals the number of valence electrons. This prescription yields a radius of 2.5 bohr for the sphere around an oxygen atom, and for the sphere around a tin atom 2.5 bohr in SnO_2, 2.75 bohr in SnO. The resulting total charges on the tin atoms are -1.15 electrons in SnO and -2.0 electrons in SnO_2, which is a reasonable estimate. In detail, in SnO_2 we obtain 0.85, 0.85, 0.25, and 0.1 for the valence electrons of tin of s, p, d, and f symmetry, respectively, whereas the corresponding results for SnO are 1.33, 1.17, 0.25, and 0.1.

It has turned out that the relaxation of the core in such a fixed configuration is not critical at all for the results. In particular, calculations performed with a core frozen in its ground state yield lattice parameters that differ from the ones obtained with the pseudopotential used in the present work (and which is, in fact, the one calculated in the configuration deduced from the analysis of SnO_2) by less than 1% . From all those results, we can estimate that it is reasonable to treat the $4d$ electrons as core electrons for the calculations of this kind of structural properties, thus validating the results that we have exposed in this work.

V. CONCLUSIONS

In conclusion, we have performed *ab initio* calculations of the ground-state properties of tin monoxide. We have shown that the cohesion of SnO can be understood in terms of interlayer screening. In spite of the resulting relatively weak interaction between the layers, we do not find particular problems linked to the use of the local-density approximation. Instead, we have discussed the importance of the choice of the local reference component of the tin pseudopotential. It emerges that, whereas it is a general finding that the local component should be chosen with care even when no problems linked to fully separable potentials arise, in the case of SnO a bad choice for the reference component can be the reason for big discrepancies with experiment. With a carefully constructed pseudopotential on the other hand, excellent results are obtained for both SnO and SnO_2.

[1] J. Watson, Sens. Actuators **5**, 29 (1984).

[2] C. Tatsuyama, S. Ichimura, and H. Iwakuro, Jpn. J. Appl. Phys., Part 2 **21**, L25 (1982).

[3] C.L. Lau and G.K. Wertheim, J. Vac. Sci. Technol. **15**, 622 (1978).

[4] P.M.A. Sherwood, Phys. Rev. B **41**, 10151 (1990).

[5] J. Robertson, J. Phys. C **12**, 4767 (1979).

[6] A. Svane and E. Antoncik, J. Phys. Chem. Solids **48**, 171 (1987).

[7] A. Svane and E. Antoncik, Phys. Rev. B **35**, 4611 (1987).

[8] I. Manassidis, J. Goniakowski, L.N. Kantorovich, and M.J. Gillan, Surf. Sci. **339**, 258 (1995).

[9] J. Goniakowski, J.M. Holender, and L.N. Kantorovich, and M.J. Gillan, Phys. Rev. B **53**, 957 (1996).

[10] Ph. Barbarat and S.F. Matar, Comput. Mater. Sci. **10**, 368 (1998).

[11] M. Meyer, G. Onida, A. Ponchel, and L. Reining, Comput. Mater. Sci. **10**, 319 (1998).

[12] P. Hohenberg and W. Kohn, Phys. Rev. **136**, B864 (1964); W. Kohn and L. Sham, Phys. Rev. **140**, A1133 (1965).

[13] N. Troullier and J.L. Martins, Phys. Rev. B **43**, 1993 (1991).

[14] D. Vanderbildt, Phys. Rev. B **41**, 7892 (1990).

[15] see, for example, V. Fiorentini, M. Methfessel, and M. Scheffler, Phys. Rev. B **47**, 13 353 (1993).

[16] W.J. Moore, and L. Pauling, J. Am. Chem. Soc. **63**, 1392 (1941).

[17] R.W.G. Wyckoff, *Crystal Structures*, 4th ed. (Interscience, New York, 1974), p. 136.

[18] D.M. Adams, A.G. Christy, J. Haines, and M.S. Clark, Phys. Rev. B **46**, 11 358 (1992).

[19] G. Bachelet, D.R. Hamann, and M. Schlüter, Phys. Rev. B **26**, 4199 (1982).

[20] L. Kleinman and D.M. Bylander, Phys. Rev. Lett. **48**, 1425 (1982).

[21] D.R. Hamann, Phys. Rev. B **40**, 2980 (1989).

[22] S. Louie, S. Froyen, and M.L. Cohen Phys. Rev. B **26**, 1738 (1982).

[23] R.W.G. Wyckoff, *Crystal Structures*, 2nd ed. (Interscience, New York, 1963), p. 251.

[24] J.F. Nye, *Physical Properties of Crystals* (Oxford University Press, New York 1985), p. 146-147.

[25] X. Gonze, P. Käckell, and M. Scheffler, Phys. Rev. B **41**, 12 264 (1990).

[26] M. Fuchs and M. Scheffler, Chem. Phys. Lett. **119**, 67 (1999).

[27] *CRC Handbook of Chemistry and Physics,* 67th ed. edited by R.C. Weast, M.J. Astle, and W.H. Beyer (CRC, Boca Raton, Florida, 1986–1987), p. D-37

[28] M.M. Choy, W.R. Cook, R.F.S. Hearmon, H. Jaffe, J. Jerphagnon, S.K. Kurtz, S.T. Liu, and D.F. Nelson, Landolt-Börnstein, *Numerical Data and Functional Relationships in Science and Technology*, New Series, Group III, Vol. 11, edited by K.-H. Hellwege and A.M. Hellwege (Springer, Berlin, 1979), p. 60.